Environmental Science Processes & Impacts

ROYAL SOCIETY OF CHEMISTRY

PAPER

View Article Online
View Journal | View Issue

Cite this: *Environ. Sci.: Processes Impacts*, 2021, **23**, 559

Emerging investigator series: chemical and physical properties of organic mixtures on indoor surfaces during HOMEChem†

Rachel E. O'Brien, *[a] Ying Li, [b] Kristian J. Kiland, [c] Erin F. Katz,‡[d] Victor W. Or, [e] Emily Legaard,[a] Emma Q. Walhout,[a] Corey Thrasher,[a] Vicki H. Grassian, [ef] Peter F. DeCarlo, [g] Allan K. Bertram[c] and Manabu Shiraiwa [b]

Organic films on indoor surfaces serve as a medium for reactions and for partitioning of semi-volatile organic compounds and thus play an important role in indoor chemistry. However, the chemical and physical properties of these films are poorly characterized. Here, we investigate the chemical composition of an organic film collected during the HOMEChem campaign, over three cumulative weeks in the kitchen, using both Fourier Transform Ion Cyclotron Resonance Mass Spectrometry (FT-ICR MS) and offline Aerosol Mass Spectrometry (AMS). We also characterize the viscosity of this film using a model based on molecular formulas as well as poke-flow measurements. We find that the film contains organic material similar to cooking organic aerosol (COA) measured during the campaign using on-line AMS. However, the average molecular formula observed using FT-ICR MS is $\sim C_{50}H_{90}O_{11}$, which is larger and more oxidized than fresh COA. Solvent extracted film material is a low viscous semisolid, with a measured viscosity $<10^4$ Pa s. This is much lower than the viscosity model predicts, which is parametrized with atmospherically relevant organic molecules, but sensitivity tests demonstrate that including unsaturation can explain the differences. The presence of unsaturation is supported by reactions of film material with ozone. In contrast to the solvent extract, manually removed material appears to be highly viscous, highlighting the need for continued work understanding both viscosity measurements as well as parameterizations for modeled viscosity of indoor organic films.

Received 1st February 2021
Accepted 7th April 2021

DOI: 10.1039/d1em00060h

rsc.li/espi

Environmental significance

Indoor surfaces become coated with a thin layer of organic material which can play an important role in indoor air quality. Very little is known about the composition of different indoor films, especially the lower volatility material that can remain on the surface for long periods of time. In this work, we show that a representative film collected in a kitchen is chemically similar to cooking organic aerosol, but it contains larger molecules. We also find that unsaturation needs to be included to correctly model the viscosity of the film. Improvements in our ability to accurately model the chemical and physical properties of indoor surface films are necessary steps towards improving models describing the chemistry occurring in different indoor environments.

[a]*Department of Chemistry, William & Mary, Williamsburg, VA, 23185, USA. E-mail: reobrien@wm.edu*

[b]*Department of Chemistry, University of California Irvine, Irvine, CA 92697, USA*

[c]*Department of Chemistry, University of British Columbia, Vancouver, British Columbia V6T 1Z1, Canada*

[d]*Department of Chemistry, Drexel University, Philadelphia, PA 19104, USA*

[e]*Department of Chemistry and Biochemistry, University of California San Diego, La Jolla, California 92093, USA*

[f]*Scripps Institution of Oceanography and Department of Nanoengineering, University of California San Diego, La Jolla, California 92093, USA*

[g]*Department of Environmental Health and Engineering, Johns Hopkins University, Baltimore, MD, 21218, USA*

† Electronic supplementary information (ESI) available. See DOI: 10.1039/d1em00060h

‡ Present address: Department of Chemistry, UC Berkeley, Berkeley, CA 94720, USA.

1 Introduction

Organic films on indoor surfaces can be formed through the deposition of semi-volatile organic compounds (SVOC) and aerosol particles.[1–5] Due to the high surface area to volume ratio indoors,[6–8] these films play important roles in the chemistry of indoor environments as a medium for chemical reactions[9] and as a location for partitioning of gas-phase molecules including SVOCs as well as ammonium and HONO.[10–16] Previous studies evaluating the chemical components of these films focused on measuring SVOCs.[5,17,18] However, many chemicals found in aerosol particles can be much lower volatility, and oligomerization reactions in the film may also decrease the volatility.[19] The chemical composition of the film will play a role in the

partitioning behaviour of gas-phase molecules and should be characterized across a range of different indoor environments to determine the most representative chemical structures for these films for indoor chemistry models.

The physical properties, such as the viscosity, of indoor organic films may also play an important role in indoor environments. For example, heterogeneous oxidation by ozone can produce volatile products,[20,21] but reactions may be spatially limited to the surface of viscous films.[22] Thus, a high film viscosity could limit the portion of the film that is available to produce volatile products from reactions with ozone. In addition, the mobility of SVOCs may decrease in viscous mixtures.[23] This can impact the timescales for equilibration when, for example, ventilation rates change in an indoor environment.

The viscosity of films can be measured with poke-flow experiments, from the time taken for the deformed material to regain its prior shape.[24–29] Recent studies have also shown that viscosities for complex organic mixtures can be estimated, as a function of relative humidity (RH) and temperature (T), from molecular formulas in the mixtures.[30–32] The modelled viscosity has been parametrized with chemicals that have functional groups and structures similar to ones found in outdoor organic aerosol particles,[30–32] but this may not fully represent the complex organic mixture found in indoor surface films.

One of the largest sources for organic material indoors is food cooking,[33] and cooking organic aerosol (COA) has been characterized with techniques such as gas chromatography/mass spectrometry (GC/MS), chemical ionization mass spectrometry (CIMS), and aerosol mass spectrometry (AMS).[34–42] GC/MS and CIMS show molecules with carbon numbers up to $\sim C_{30}$ from COA samples.[37,43] In an AMS, COA is characterized by high abundances at m/z 41 ($C_3H_5^+$), 43 ($C_3H_7^+$ and $C_2H_3O^+$), 55 ($C_4H_7^+$ and $C_3H_3O^+$), and 57 ($C_4H_9^+$ and $C_3H_5O^+$).[34,35,41,43] Overall, COA has a relatively low oxygen to carbon ratio (O/C) ranging from $\sim$0.1 to $\sim$0.2 to 0.3 for fresh and more aged COA, respectively.[35] Indoors, COA particles and SVOCs from food cooking can deposit onto surfaces forming an organic film. Once on the surface, the chemical and physical properties of this mixture may continue to evolve *via* mechanisms like heterogeneous oxidation or oligomerization.[11,44]

To improve our ability to model indoor air quality and indoor exposure to chemicals, a more complete characterization of the chemical and physical properties of organic films on indoor surfaces is needed. This will provide important constraints for modelling efforts targeting the chemical reactions that occur on indoor surfaces as well as the distribution of SVOC compounds in different indoor environments. The objective of this study was to fully characterize these properties for a film collected and aged for three weeks during the 2018 House Observations of Microbial and Environmental Chemistry (HOMEChem) campaign.[33]

Here, the chemical properties of an extract of this film were measured using two different mass spectrometry techniques: one that provides a direct comparison with aerosol particles measured *in situ* and one that provides molecular properties of the chemicals in the film. The viscosity of the film extract was measured with a poke-flow technique and was compared to the viscosity modelled using the molecular composition. To provide a broader context for the characteristics of the aged film, comparisons were also made to an independent sample of deposited material that was collected for a shorter duration during the same field campaign and was analysed with a microscopy technique.

This combination of techniques shows that the extract of the film had chemical properties similar to COA, but with higher molecular weights. The modelled viscosity was high, but matched the lower observed viscosity when double bonds were included in the parameterization. These viscosity results are all in contrast to observations of the film when it was manually removed: this material was a crumbly solid. Overall, the results presented here demonstrate that (1) very large molecules can be found deposited on indoor surfaces, (2) updated model parameterizations are needed for indoor organic film viscosity, and (3) solvent extraction and longer-term aging can both modify the observed physical properties of indoor organic films.

2. Materials and methods

In this study, two types of samples were analysed. The first sample was a film that formed over three weeks and the majority of the information in this section refers to this sample. The second sample was deployed for a shorter duration (4 days) and this sample is described below at the end of Section 2.3.

2.1 Sample collection/preparation

Details on the HOMEChem campaign are provided in Farmer and Vance *et al.* (2019).[33] Briefly, experiments that replicate typical indoor activities, including cooking, were carried out over $\sim$one month in the University of Texas at Austin's Test House. Ozone concentrations were fairly consistent with mixing ratios indoors of $\sim 8 \pm 18$ ppb. During the last three weeks (June 10, 2018 to June 29, 2018) two glass plates were deployed in the kitchen above the stove, placed at a steep slant ($\sim$85°) (Fig. S2†). Field blank plates were opened for $\sim$5 min in the kitchen and then resealed and stored in their bag against the wall for the same time period.

Prior to deployment, glass plates intended for MS analyses were cleaned using 4–5 rinses with Milli-Q water (18 MΩ, Millipore Sigma) followed by a rinse with methanol and were dried in a hood. After deployment, the exposed sides of the glass were pressed against each other and the plates were wrapped in aluminium foil, placed in a plastic bag, and then placed in a brown padded shipping bag for transport. Samples were stored frozen at -20 °C except during a flight ($\sim$12 hours). No ice packs were used during the flight due to airline and weight restrictions. However, we note that the glass plates are fairly thick and take $\sim$3 hours to thaw when placed in sets of two (one pack) on the lab bench. The stack of 8 sets of plates still felt cool when it was placed in the freezer at the end of the trip. This small bit of warming may have changed some chemical properties compared to what was collected after three weeks of deployment at HOMEChem; however, we expect a few hours at

a cool temperature in a closed container will have a minimal impact.

Two methods for sample removal were used here. In the first, solvent extraction of organic material was carried out using a novel surface extractor which consists of a 0.5″ (1.3 cm) Teflon tube filled with acetonitrile (5 mL total in ~1 to 2 mL increments). This tube was pressed down onto the surface and moved around in a circle of ~3″ (7.7 cm) diameter. The material that dissolved in the acetonitrile was collected from the surface *via* a 1/8″ (0.3 cm) Teflon line into a clean collection vial using a vacuum pump; a full characterization of the extractor is in preparation. The same method was used to collect the field blank using a separate set of Teflon tubing. Extracted samples were dried under a gentle stream of ultra-high purity nitrogen (UHP N_2) and were stored at −20 °C until analysis.

The second method of sample removal involved scraping a cleaned razor blade across the surface. This built up small waxy clumps of the film on the edge of the blade that were then placed into a small glass vial. Analysis of the physical properties of this manually removed material is ongoing; the description provided here comes from the observed behaviour when a sample was pressed down onto an Attenuated Total Reflectance-Fourier Transform Infrared spectroscopy crystal for Or *et al.* (2020).[2] The total area that was scraped with the razor blade was approximately the same as the solvent extraction.

For the ozone reaction experiment, approximately one third of an acetonitrile extract was dried under UHP N_2 in the bottom of a 20 mL glass vial. This open vial was then placed in a gas-tight box with ~2 L min^{-1} of zero air and ~3 ppm ozone flowing through. Ozone was produced using a Penray lamp (Model 600, Jelight Co. Inc.) and the ozone concentration was measured using a 2B Technologies UV absorption ozone meter. The vial was exposed to ozone in the box for 24 hours at room temperature and then stored at −20 °C until analysis.

2.2 Mass spectrometry

For offline AMS analysis, one third of the acetonitrile extract was dried and reconstituted with 50 μL Milli-Q water and atomized into a High Resolution-Time of Flight-Aerosol Mass Spectrometer (HR-AMS)[45,46] using the small volume nebulizer (SVN).[47] The spectrum for the field blank was spectrally subtracted from the sample spectrum after weighting the field blank intensities by a factor of 0.2. The resulting electron ionization (EI) mass spectral data was analysed using software packages SQUIRREL (v1.57I) and PIKA (v1.16I).

A separate HR-AMS was used during HOMEChem to make online measurements of sub-micron non-refractory aerosol.[46,48] Data utilized in this work includes high resolution organic aerosol mass spectra up to m/z 100 averaged over the same time period that the glass plates were deployed. The AMS inlet was located in the test house kitchen adjacent to the refrigerator, and the sample air was dried prior to analysis by the AMS. Additional HR-AMS details are presented in Katz *et al.* (2021).[49] Because small fragments are produced in the AMS detection scheme, high-resolution organic aerosol data was analysed only up to m/z 100. O/C and H/C calculations were performed following the method of Canagaratna *et al.* (2015) which was the same method used for offline AMS analysis.[50]

Electrospray ionization Fourier Transform-Ion Cyclotron Mass Spectrometry (ESI FT-ICR MS) was carried out using electrospray ionization of the two samples (unreacted and aged with ozone) on a Bruker Daltonics 12 Tesla Apex Qe at Old Dominion University. About one third of the dried extract samples were reconstituted with methanol (~300 μL), diluted by a factor of 200 with methanol, and sprayed in positive ion mode. Assignments were made using methods similar to previous work[47,51] with a mass accuracy window of 1 ppm, the molecular formula calculator (https://nationalmaglab.org/user-facilities/icr/icr-software), and a range of values $C_{0-100}H_{0-200}O_{0-50}N_{0-3}Na_{0-1}$. For the FT-ICR MS analysis, any peaks observed in the field blank were removed from the final sample peak list.

2.3 Viscosity

The viscosity of the organic material in the film was predicted using the measured elemental composition from FT-ICR MS analysis following the parameterization in DeRieux and Li *et al.* (2018) using compounds containing carbon, hydrogen, and oxygen. Eqn (1) was applied to estimate the glass transition temperature (T_g) of individual compounds:

$$T_{g,i} = (n_C^0 + \ln(n_C))b_C + \ln(n_H)b_H + \ln(n_C)\ln(n_H)b_{CH} + \ln(n_O)b_O + \ln(n_C)\ln(n_O)b_{CO} \quad (1)$$

where n_C, n_H, and n_O are the number of carbon, hydrogen, and oxygen atoms, respectively. Values of the coefficients [n_C^0, b_C, b_H, b_{CH}, b_O, and b_{CO}] are [12.13, 10.95, −41.82, 21.61, 118.96, −24.38] as used previously.[30] The glass transition temperature of the dry organic mixture ($T_{g,org}$) is calculated by the Gordon–Taylor equation with the Gordon–Taylor constant (k_{GT}) of 1:[52] $T_{g,org} = \sum_i w_i T_{g,i}$. The mass fraction w_i is assumed to be proportional to the relative abundance in the mass spectrum. The predicted $T_{g,org}$ is very high (422 K), reflecting that the majority (97%) of the detected compounds have high molar mass (>500 g mol^{-1}) as discussed in the text. The RH in the kitchen was between 43% to 82%, with an average of 57%,[33] leading to water uptake by organic films. The mass fraction of water was estimated using the effective hygroscopicity parameter (κ).[53] κ was not measured during the HOMEChem campaign, so we assumed a value of 3×10^{-3} or 0.14 estimated for fresh or aged COA, respectively.[54] T_g of a mixture of organics and water ($T_{g,mix}$) can be calculated by the Gordon–Taylor equation with k_{GT} of 2.5.[55] Using the calculated $T_{g,mix}$, the temperature-dependence of viscosity can be calculated applying the Vogel–Tammann–Fulcher (VTF) equation.[30,56,57]

The viscosity of the HOMEChem extract samples was measured using the poke-flow technique.[24–29] For these experiments, a separate replicate acetonitrile extraction was carried out. The poke-flow technique has been developed to measure the viscosity of small samples (~1 mg of material) with values ranging from 10^8 Pa s to less than 10^4 Pa s. Details on the approach used here as well as representative movies of some experiments are provided in the ESI.†

A full description of the method for sample collection and analyses for Atomic Force Microscopy (AFM) is available in Or *et al.* (2020).[2] Briefly, 1.3 × 1.3 cm pieces of glass were cleaned with methanol and water rinses and were placed vertically in the kitchen and shared living room of the Test House. Samples were exposed for four days (June 24, 2018 to June 28, 2018) before transfer to sealed stainless-steel containers. Samples were stored in the dark at ambient conditions and analysed under ambient conditions.

3. Results and discussion

3.1 Aerosol mass spectrometry

Cooking events during HOMEChem produced high particle concentrations ranging from ~20 to 350 μg m^{-3} with the largest concentrations during stir fry, breakfast, and chili cooking.[33] Online AMS measurements showed variations in the mass spectra during different cooking activities.[33] Since the plates were deployed for three cumulative weeks, the film is likely an average of gases and particles that deposited during that time.

Fig. 1a shows the offline HR-AMS mass spectrum for the material extracted off the glass surface and Fig. 1b shows the average on-line HR-AMS mass spectrum over the same time period. The signal for N-containing ions was very low in both AMS data sets (N/C ~0.005 for offline AMS); thus only identified ions containing carbon with hydrogen and/or oxygen atoms (*e.g.* C_xH_y or $C_xH_yO_z^+$ fragments) are included for analysis. Both mass spectra are similar to COA observed in the field,[41,58,59] with high abundances at *m/z* 41 ($C_3H_5^+$), 43 ($C_3H_7^+$ and $C_2H_3O^+$), 55 ($C_4H_7^+$ and $C_3H_3O^+$), and 57 ($C_4H_9^+$ and $C_3H_5O^+$). The weighting between ions found at the same nominal mass can be seen in the relative heights of the stacked green *vs.* purple bars in Fig. 1.

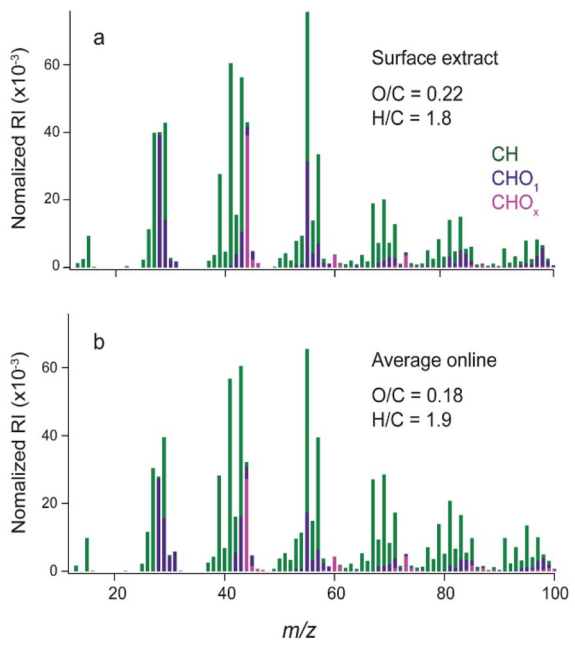

Fig. 1 AMS mass spectra for the C, H, and O containing ions in the (a) aqueous solution of surface extract, (b) average online AMS spectrum during the same time period at HOMEChem. Spectra are plotted showing the types of MS fragments found at each *m/z* (with CH = no oxygen atoms, CHO_1 = one oxygen, and CHO_x = greater than one oxygen in the formula). Average ensemble properties are given next to each mass spectrum.

The two AMS mass spectra have similar overall fragmentation patterns with a dot product between them of 0.97. To evaluate the similarity for lower abundance ions, the log of each of the intensities was also taken and the corresponding dot product was 0.74. These results suggest that there is a high degree of chemical similarity between the samples, but that there are differences in the lower abundance ions. This is expected given the differences in age between the samples and the potential for solubility to influence the composition of the extract.

The largest difference between the two mass spectra is that the surface extract is slightly more oxidized, with an average O/C of 0.22 compared to 0.18 for the online AMS. The higher O/C may be due to the fact that the extract is the water-soluble fraction. In addition, during the three-week deployment the material was exposed to oxidants such as ozone and OH radicals which may have oxidized the organic mixture, as well as to VOCs and SVOCs which may have oligomerized into the film. The good agreement between offline and online AMS spectra in Fig. 1 demonstrates that COA, and likely SVOCs associated with COA, make up a large fraction of the material that deposited on nearby surfaces in the kitchen during HOMEChem.

3.2 FT-ICR MS

Additional information about the chemical mixture can be gained using soft ionization mass spectrometry to characterize larger, intact molecular ions. Fig. 2a shows an ESI FT-ICR MS mass spectrum for carbon-, hydrogen-, and oxygen-containing compounds in the extract. In Fig. 2b, the double bond equivalence (DBE) *vs.* the *m/z* is shown and the inset in Fig. 2a shows the Van Krevelen plot for these ions. This manuscript focuses on the C, H, and O containing ions because, as mentioned above, the amount of nitrogen observed in the offline AMS was very low (N/C = 0.005). Fig. S3† shows the full FT-ICR MS mass spectrum for the unreacted sample with some nitrogen containing ions. These are likely trace amounts of compounds with reduced nitrogen such as amines which can have very high ionization efficiency in ESI and thus be over-represented in terms of abundance.

In this extract, 243 molecular formulae were identified with an average molecular weight of ~840 atomic mass units (amu). The average intensity weighted molecular formula is $C_{50}H_{90}O_{11}$, which has the same O/C ratio (0.22) as the average offline AMS (Fig. 1a). This suggests that both mass spectrometers are measuring a similar chemical mixture, despite the differences in the solvents used (Milli Q water *vs.* methanol).

Previous studies have shown that online AMS mass spectra during HOMEChem stir fry experiments compared well with aerosolized vegetable (soy) oil emitted in a test house kitchen.[33] The center of the mass range from the FT-ICR MS analysis of the extract is similar to triglycerides in soy oil (~900 amu), as is the DBE distribution, while the extract is more oxidized than pure

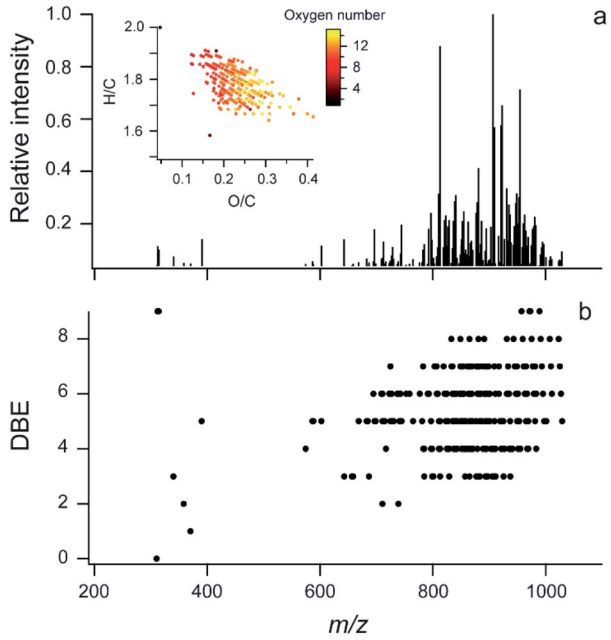

Fig. 2 Soft ionization mass spectra. (a) ESI FT-ICR data for CHO compounds in glass surface extracts, inset is the Van Krevelen plot with markers coloured by the number of oxygen atoms in the molecule; two molecules are off scale (see Fig. S3b†). (b) DBE *vs.* *m/z* for the same sample.

triglycerides (O/C ~ 0.1).[60] In the higher mass region, the DBE ranges from ~3 to 9. These double bond equivalents can be carbon–carbon double bonds (C=C), carbon–oxygen double bonds (C=O), or rings. If chemicals like triglycerides are present, some of these double bonds are likely esters, but there is also the possibility of unsaturation or rings.

The chemical mixture shown in Fig. 2 is primarily comprised of large molecules, but COA has also been found to contain smaller molecules (~C_{30} and less).[37,43] The lack of smaller molecules in this sample may be partially explained by the analytical methods used here because the sample was evaporated under UHP N_2. It is also possible that some SVOCs reacted with material in the film, forming oligomers with higher molecular weight.

The number of different molecular formulae and the higher O/C suggest a more complex mixture is present on the surface than a mixture of different triglycerides. This is consistent with increased oxygen content in COA when vegetables and sauce are added to a stir-fry[33] and may also indicate that reactions occurred in the film over the three week deployment. Overall, the molecules found on this surface are too large and likely have too low volatility to be measured by GC/MS; thus, the use of FT-ICR MS provides a first look at these lower volatility components on an indoor surface.

3.3 Physical properties

Chemical composition can affect the viscosity of organic films and this viscosity is important to understand because it can play a role in the sorption behaviour of SVOCs. Using the molecular formulas in Fig. 2, the predicted viscosity, as a function of RH at room temperature, is shown as the purple shaded area in Fig. 3a, using estimates for the $T_{g,org}$ of 422 K. The upper and lower boundary lines of the shaded area are calculated with κ of 0.003 and 0.14, respectively. During HOMEChem, the RH in the kitchen reached as high as 82%,[33] but tended to range from ~40 to 60% leading to a predicted semi-solid or solid phase in this aged organic material (10^6 to 10^{12} Pa s).

In contrast with the predicted values, Fig. 3a also shows viscosity ranges from poke-flow measurements of the extracted material (black circles and arrows). For all RH values studied, the measured viscosities are less than 10^4 Pa s (black dots with downward arrows). This viscosity is in the range of peanut butter (~10^4 Pa s) or honey (~10 Pa s)[61] and the mixture is a low viscous semi-solid. The much higher viscosity predicted using the initial estimates for $T_{g,org}$ (purple shaded area) indicates a large measurement/model gap for this material.

The low measured viscosity for deposited organic material is also supported by imaging analysis. Fig. 3b shows AFM images of particles collected over four days at the end of the campaign on a separate glass plate and Fig. 3c shows the distribution of aspect ratios. Flatter particles with a low aspect ratio were observed suggesting that the freshly deposited particles on this surface have a low viscosity.[2]

For the modelled viscosity, eqn (1) estimates the model parameter, T_g, based only on chemical composition and was derived from a dataset mostly with saturated compounds comprising OH and COOH functional groups.[55,57] While this method has been successful in predicting viscosity of atmospheric SOA,[30,31] it could significantly overestimate the T_g of compounds containing carbonyl and ester groups.[31] Molecular structure and functional groups have a close relationship with viscosity,[28,57] which is not explicitly considered in the applied parameterization.

Given the similarities to COA and triglycerides in the mass spectral analysis, the presence of unsaturation should be considered in this mixture. Unsaturated fatty acids are known to have lower melting points than saturated fatty acids: the presence of one or more double bonds results in bends in the hydrocarbon chain, making molecules harder to stack together with weaker intermolecular interactions, lowering the melting point and T_g.[62] Table S1 and Fig. S4† show that T_g of triglycerides could be significantly overestimated by ~155 K to 245 K, depending on DBE, with higher DBE leading to larger overestimation. Sensitivity simulations correcting the effects of DBE (ESI†) show that the predicted $T_{g,org}$ of the surface extract could decrease from 422 K to 236 K, giving a predicted viscosity lower than 10^3 Pa s, which is within the range of measured viscosities (Fig. 3a, pink shaded). This indicates that including structural information in estimating T_g[63] can help improve model performance and reduce the uncertainty in the predicted viscosity of indoor organic films.

Taken together, these results show that acetonitrile extracts from the HOMEChem surface are a low viscous semi-solid, and that including double bonds closes the gap between the modelled and measured viscosities (Fig. 3a). The comparison with AFM results (Fig. 3b and c) is consistent with this view,

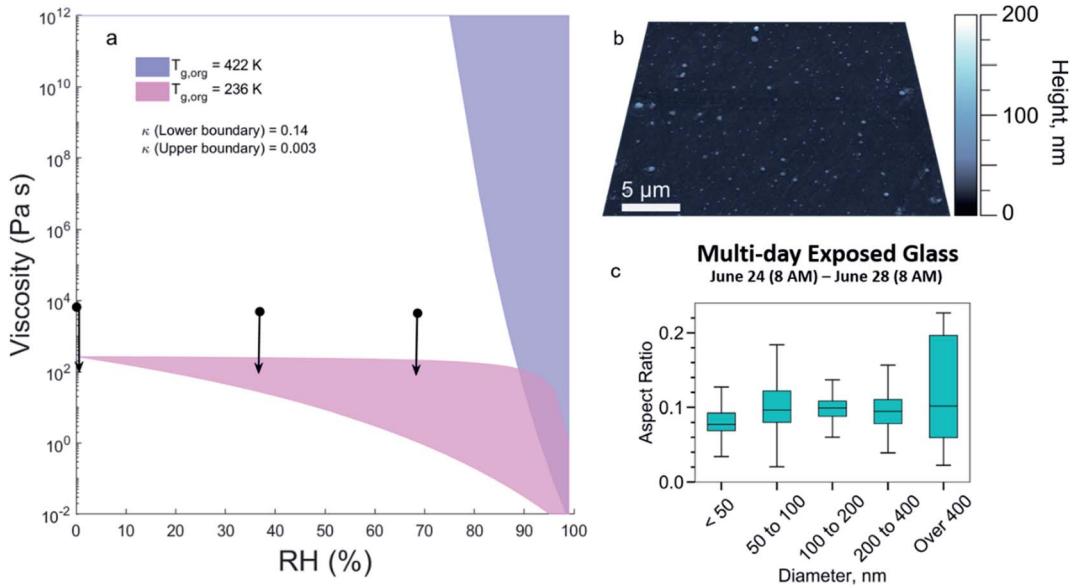

Fig. 3 (a) Viscosities of the organic matter (OM) deposited near the stove. The blue and pink shaded areas represent the viscosity with $T_{g,org}$ of 422 K, predicted with original T_g parameterizations, and of 236 K, predicted by accounting for the presence of double bonds, respectively. The upper and lower boundary lines of the purple or pink shaded areas are calculated with the hygroscopicity parameter (κ) of 0.003 and 0.14 (Li *et al.*, 2018), respectively. Measured viscosity is shown by black circles and arrows. (b) and (c) results from AFM analysis of a shorter duration sample deployed during the end of the sampling period. (b) shows the 3D height images and (c) the aspect ratio measured for different size bins.

showing that a lower viscosity is also observed in the freshly deposited particles.

However, the same sample was used for a prior study (Or *et al.* (2020)[2]) and film material was removed from the surface in a different area of the glass using a razor blade, as described above in Section 2.1. The observed viscosity of the manually scraped material was much higher (Fig. S5†). The scraped material appeared more solid, and it crumbled when pressed. The apparent viscosity of the freshly deposited material (Fig. 3b and c) can be compared with this three week aged, manually removed material. The higher viscosity of the scraped material, compared with the low aspect ratio of freshly deposited particles (Fig. 3b and c), suggests that longer term aging can increase the viscosity of indoor organic films. Possible mechanisms include the loss of smaller molecules (decreased plasticization), oligomerization, or increased intermolecular bonding through increased oxidation. We highlight that this increase in viscosity with aging also matches everyday experiences; for example, thicker organic films on kitchen surfaces often become more difficult to remove after a few days or weeks. The viscosity of the manually removed material could not be determined from the poke-flow technique and ongoing work is being carried out to determine the viscosity of this material as well as the effects of solvent extraction on the physical properties of indoor surface films.

3.4 Ozonolysis

The above analyses demonstrate that the presence of carbon–carbon double bonds (C=C) closes the observed gap between the measured and modelled viscosity. Further support for the presence of double bonds in the mixture is provided by an experiment exposing a portion of the dried acetonitrile extract to high concentrations of ozone, which can react with unsaturated carbon.

Fig. 4a shows results from ESI FT-ICR MS analysis with the unreacted sample in black and the sample exposed to 3 ppm ozone for 24 hours overlaid in blue; the inset shows the change in a Van Krevelen diagram. Overall, ozonolysis leads to fragmentation and some oxidation of the mixture with increases in the average intensity weighted O/C from 0.21 to 0.24 and decreases in the average, intensity-weighted carbon number from 50 to 46. Molecules that are not detected in the FT-ICR MS for the sample exposed to ozone are indicated by black peaks without a blue peak overlaid on top (Fig. 4a). This loss is observed across the mass spectrum and especially in a group around 850–1000 *m*/*z*. In the Van Krevelen inset, these peaks are dominantly found in the lower H/C and O/C region. After ozonolysis, there are a few molecules that have high O/C (>0.5), these molecules have an average molecular weight around 600 amu and a formula $\sim C_{26}H_{51}O_{14}$.

Removal of peaks in the mass spectrum suggests chemical transformations and/or fragmentation reactions occurred, changing the molecular composition. However, the mass spectrum for the ozone sample has only a few new, smaller mass ions after aging. The lack of smaller fragment ions may be due to some material volatilizing out of the samples during the aging process. It is important to note that this analysis probes the molecular formulas only and the intensities are not quantitative; chemical transformations can change the formulas to ones already present in the sample, giving the appearance of a lack of reaction. Overall, 86 common molecular formulas were found with 82 unique formulas for the ozonolysis sample and

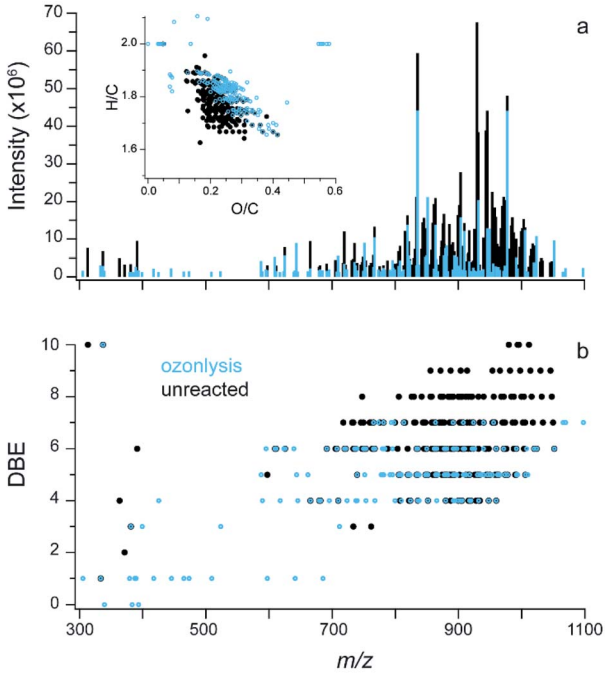

Fig. 4 Soft ionization mass spectra of unreacted (black) and ozonolysis (blue) samples. (a) ESI FT-ICR data with absolute intensity for CHO compounds in glass surface extracts, (b) DBE *vs.* *m*/*z*. The sample exposed to ozonolysis is shown as open circles in (b) to aid visualization.

157 unique for the unreacted. Future experiments will probe the composition of the gas-phase species that evolve off similar indoor films when exposed to ozone as well as chromatography based chemical analysis of aged indoor films.

To further illustrate the role of double bonds, Fig. 4b shows the DBE plotted *vs.* *m*/*z* for unreacted material (black) and ozonolysis (blue) overlaid on top. After ozonolysis, most of the molecules containing 7 to 10 double bonds were removed. The average intensity weighted DBE changed from 6.0 to 5.0 after ozonolysis. The number of carbon–carbon double bonds per molecule cannot be probed with this experiment, necessitating the sensitivity analysis described above. However, this aging experiment provides an indirect probe for the presence of C=C in some of the molecules in the mixture and supports the inclusion of unsaturation in the parameterization of the viscosity model.

The ozonolysis aging experiment also shows that the deposited material could act as an ozone sink indoors. As discussed above, this extract has some fluid properties (Fig. 3a), but the observed viscosity of the manually removed material appears to be higher (Fig. S5†). This is consistent with a recent study which indicated that organic film materials collected in a kitchen are highly viscous.[64] The higher viscosity of the intact film may slow heterogeneous chemistry such as ozone reactions with C=C bonds and heterogeneous NO_2 conversion to HONO. The concentration of ozone in the house was, on average, fairly low: ~8 ± 18 ppb.[33] This, combined with the higher observed viscosity of the manually removed film, may explain why there were still C=C bonds in the film after three weeks exposure/deposition in the test house. The reactivity shown in Fig. 4 is likely an upper estimate of the total uptake that could occur if the film was exposed to a high concentration of ozone. Future work is needed to characterize the extent that intact films similar to this can act as sinks for indoor ozone.

4. Conclusions

This work is the first analysis of higher molecular weight compounds on indoor surfaces. The material on the surface has chemical properties that are very similar to COA particles measured online with an AMS over the same time period. The good agreement between the offline and online AMS data sets demonstrates the capability for offline AMS analysis of surface films to provide insights into important sources; this will become especially relevant as more online AMS datasets for indoor aerosol particles are collected.

The viscosity of organic films on indoor surfaces can influence the type of chemical reactions that occur on the surface as well as the partitioning of SVOCs indoors. This study is the first direct measurement of the viscosity of extracted film material off indoor surfaces and it provides a starting point for indoor models that include the physical properties of the films in predicting the concentration of SVOCs indoors. The comparison between measured and modelled viscosities shows that the extracted sample is a low viscous semi-solid and that the chemicals deposited in this kitchen contain unsaturation which should be included in the model parameterization for surface films from COA. The addition of unsaturation into the model closes the measurement/model gap for the extracted material. However, the higher observed viscosity for the scraped material compared to the freshly deposited particles indicates remaining gaps in the parameterization of the modelled viscosity for aged indoor films. It also demonstrates gaps in our understanding of how longer-term aging affects the physical properties of indoor organic films and on how solvent extractions influence the measured viscosity of indoor films. Future studies are needed to probe the evolution of the chemical and the physical properties of indoor organic films in kitchens as well as in other indoor spaces to improve our ability to model and predict indoor air quality and the chemistry of different indoor environments.

Author contributions

The manuscript was written through contributions of all authors. R. E. O. collected samples and C. T. and E. L. assisted with data analysis of FT-ICR MS data; E. F. K. and P. F. D. contributed online AMS analysis; V. W. O and V. H. G. contributed AFM analysis; Y. L. and M. S. carried out modelling analysis; K. J. K. and A. K. B. carried out viscosity analysis. All authors have given approval to the final version of the manuscript.

Conflicts of interest

There are no conflicts to declare.

Acknowledgements

We thank the HOMEChem science team and Delphine Farmer and Marina Vance for all the work carried out to design and run the experiments during the campaign. The authors thank Michael Wade and Richard L. Corsi for collecting glass samples, and Atila Novoselac for RH and T measurements. We thank the Alfred P. Sloan Foundation for support G-2018-11031 (R. E. O.); G-2019-12306 and G-2020-13912 (M. S.); G-2020-12675 (V. H. G.); G-2019-12301 (P. F. D.). R. E. O. thanks Dr Deepti Varma and COSMIC (College of Sciences Major Instrumentation Cluster) for FT-ICR data, Jesse H. Kroll for HR-AMS access, and Hannah Przelomski for assistance in extracting the sample, A. K. B. and K. K. thank the Natural Science and Engineering Research Council of Canada (grant RGPIN/04315-2014).

References

1 Q.-T. T. Liu, R. Chen, B. E. McCarry, M. L. Diamond and B. Bahavar, Characterization of Polar Organic Compounds in the Organic Film on Indoor and Outdoor Glass Windows, *Environ. Sci. Technol.*, 2003, **37**, 2340–2349.

2 V. W. Or, M. Wade, S. Patel, M. R. Alves, D. Kim, S. Schwab, H. Przelomski, R. O'Brien, D. Rim, R. L. Corsi, M. E. Vance, D. K. Farmer and V. H. Grassian, Glass surface evolution following gas adsorption and particle deposition from indoor cooking events as probed by microspectroscopic analysis, *Environ. Sci. Process. Impacts*, 2020, **22**, 1698–1709.

3 Y. Wu, C. M. A. Eichler, W. Leng, S. S. Cox, L. C. Marr and J. C. Little, Adsorption of Phthalates on Impervious Indoor Surfaces, *Environ. Sci. Technol.*, 2017, **51**, 2907–2913.

4 V. W. Or, M. R. Alves, M. Wade, S. Schwab, R. L. Corsi and V. H. Grassian, Crystal Clear? Microspectroscopic Imaging and Physicochemical Characterization of Indoor Depositions on Window Glass, *Environ. Sci. Technol.*, 2018, **5**, 514–519.

5 C. M. Butt, M. L. Diamond, J. Truong, M. G. Ikonomou and A. F. H. Ter Schure, Spatial Distribution of Polybrominated Diphenyl Ethers in Southern Ontario As Measured in Indoor and Outdoor Window Organic Films, *Environ. Sci. Technol.*, 2004, **38**, 724–731.

6 A. Manuja, J. Ritchie, K. Buch, Y. Wu, C. M. A. Eichler, J. C. Little and L. C. Marr, Total surface area in indoor environments, *Environ. Sci. Process. Impacts*, 2019, 1384–1392.

7 B. C. Singer, A. T. Hodgson, T. Hotchi, K. Y. Ming, R. G. Sextro, E. E. Wood and N. J. Brown, Sorption of organic gases in residential rooms, *Atmos. Environ.*, 2007, **41**, 3251–3265.

8 C. J. Weschler and W. W. Nazaroff, Semivolatile organic compounds in indoor environments, *Atmos. Environ.*, 2008, **42**, 9018–9040.

9 A. P. Ault, V. H. Grassian, N. Carslaw, D. B. Collins, H. Destaillats, D. J. Donaldson, D. K. Farmer, J. L. Jimenez, V. F. McNeill, G. C. Morrison, R. E. O'Brien, M. Shiraiwa, M. E. Vance, J. R. Wells and W. Xiong, Indoor Surface Chemistry: Developing a Molecular Picture of Reactions on Indoor Interfaces, *Chem*, 2020, **6**, 1–16.

10 D. M. Lunderberg, K. Kristensen, Y. Tian, C. Arata, P. K. Misztal, Y. Liu, N. Kreisberg, E. F. Katz, P. F. DeCarlo, S. Patel, M. E. Vance, W. W. Nazaroff and A. H. Goldstein, Surface Emissions Modulate Indoor SVOC Concentrations through Volatility-Dependent Partitioning, *Environ. Sci. Technol.*, 2020, **54**, 6751–6760.

11 C. J. Weschler and W. W. Nazaroff, Growth of organic films on indoor surfaces, *Indoor Air*, 2017, **27**, 1101–1112.

12 L. Ampollini, E. F. Katz, S. Bourne, Y. Tian, A. Novoselac, A. H. Goldstein, G. Lucic, M. S. Waring and P. F. DeCarlo, Observations and Contributions of Real-Time Indoor Ammonia Concentrations during HOMEChem, *Environ. Sci. Technol.*, 2019, **53**, 8591–8598.

13 D. B. Collins, R. F. Hems, S. Zhou, C. Wang, E. Grignon, M. Alavy, J. A. Siegel and J. P. D. Abbatt, Evidence for Gas-Surface Equilibrium Control of Indoor Nitrous Acid, *Environ. Sci. Technol.*, 2018, **52**, 12419–12427.

14 K. Kristensen, D. M. Lunderberg, Y. Liu, P. K. Misztal, Y. Tian, C. Arata, W. W. Nazaroff and A. H. Goldstein, Sources and dynamics of semivolatile organic compounds in a single-family residence in northern California, *Indoor Air*, 2019, **29**, 645–655.

15 D. M. Lunderberg, K. Kristensen, Y. Liu, P. K. Misztal, Y. Tian, C. Arata, R. Wernis, N. Kreisberg, W. W. Nazaroff and A. H. Goldstein, Characterizing Airborne Phthalate Concentrations and Dynamics in a Normally Occupied Residence, *Environ. Sci. Technol.*, 2019, **53**, 7337–7346.

16 C. Wang, D. B. Collins, C. Arata, A. H. Goldstein, J. M. Mattila, D. K. Farmer, L. Ampollini, P. F. DeCarlo, A. Novoselac, M. E. Vance, W. W. Nazaroff and J. P. D. Abbatt, Surface reservoirs dominate dynamic gas-surface partitioning of many indoor air constituents, *Sci. Adv.*, 2020, **6**, 1–11.

17 C.-Y. Huo, L.-Y. Liu, Z.-F. Zhang, W.-L. Ma, W.-W. Song, H.-L. Li, W.-L. Li, K. Kannan, Y.-K. Wu, Y.-M. Han, Z.-X. Peng and Y.-F. Li, Phthalate Esters in Indoor Window Films in a Northeastern Chinese Urban Center: Film Growth and Implications for Human Exposure, *Environ. Sci. Technol.*, 2016, **50**, 7743–7751.

18 L. A. Wallace, W. R. Ott, C. J. Weschler and A. C. K Lai, Desorption of SVOCs from Heated Surfaces in the Form of Ultrafine Particles, *Environ. Sci. Technol.*, 2016, **51**, 1140–1146.

19 J. H. Kroll and J. H. Seinfeld, Chemistry of secondary organic aerosol: Formation and evolution of low-volatility organics in the atmosphere, *Atmos. Environ.*, 2008, **42**, 3593–3624.

20 G. Morrison, Recent Advances in Indoor Chemistry, *Curr. Sustainable Energy Rep.*, 2015, **2**, 33–40.

21 A. Wisthaler and C. J. Weschler, Reactions of ozone with human skin lipids: Sources of carbonyls, dicarbonyls, and hydroxycarbonyls in indoor air, *Proc. Natl. Acad. Sci. U. S. A.*, 2010, **107**, 6568–6575.

22 S. Zhou, B. C. H. Hwang, P. S. J. Lakey, A. Zuend, J. P. D. Abbatt and M. Shiraiwa, Multiphase reactivity of polycyclic aromatic hydrocarbons is driven by phase

separation and diffusion limitations, *Proc. Natl. Acad. Sci. U. S. A.*, 2019, **116**, 11658–11663.

23 Y. Li and M. Shiraiwa, Timescales of secondary organic aerosols to reach equilibrium at various temperatures and relative humidities, *Atmos. Chem. Phys.*, 2019, **19**, 5959–5971.

24 J. W. Grayson, M. Song, M. Sellier and A. K. Bertram, Validation of the poke-flow technique combined with simulations of fluid flow for determining viscosities in samples with small volumes and high viscosities, *Atmos. Meas. Tech.*, 2015, **8**, 2463–2472.

25 J. W. Grayson, Y. Zhang, A. Mutzel, L. Renbaum-Wolff, O. Böge, S. Kamal, H. Herrmann, S. T. Martin and A. K. Bertram, Effect of varying experimental conditions on the viscosity of α-pinene derived secondary organic material, *Atmos. Chem. Phys.*, 2016, **16**, 6027–6040.

26 M. Song, P. F. Liu, S. J. Hanna, Y. J. Li, S. T. Martin and A. K. Bertram, Relative humidity-dependent viscosities of isoprene-derived secondary organic material and atmospheric implications for isoprene-dominant forests, *Atmos. Chem. Phys.*, 2015, **15**, 5145–5159.

27 M. Song, P. F. Liu, S. J. Hanna, R. A. Zaveri, K. Potter, Y. You, S. T. Martin and A. K. Bertram, Relative humidity-dependent viscosity of secondary organic material from toluene photo-oxidation and possible implications for organic particulate matter over megacities, *Atmos. Chem. Phys.*, 2016, **16**, 8817–8830.

28 J. W. Grayson, E. Evoy, M. Song, Y. Chu, A. Maclean, A. Nguyen, M. A. Upshur, M. Ebrahimi, C. K. Chan, F. M. Geiger, R. J. Thomson, A. K. Bertram and A. Bertram, The effect of hydroxyl functional groups and molar mass on the viscosity of non-crystalline organic and organic-water particles, *Atmos. Chem. Phys.*, 2017, **17**, 8509–8524.

29 L. Renbaum-Wolff, J. W. Grayson, A. P. Bateman, M. Kuwata, M. Sellier, B. J. Murray, J. E. Shilling, S. T. Martin and A. K. Bertram, Viscosity of α-pinene secondary organic material and implications for particle growth and reactivity, *Proc. Natl. Acad. Sci. U. S. A.*, 2013, **110**, 8014–8019.

30 W.-S. Wong Derieux, Y. Li, P. Lin, J. Laskin, A. Laskin, A. K. Bertram, S. A. Nizkorodov and M. Shiraiwa, Predicting the glass transition temperature and viscosity of secondary organic material using molecular composition, *Atmos. Chem. Phys.*, 2018, **18**, 6331–6351.

31 Y. Li, D. A. Day, H. Stark, J. L. Jimenez and M. Shiraiwa, Predictions of the glass transition temperature and viscosity of organic aerosols from volatility distributions, *Atmos. Chem. Phys.*, 2020, **20**, 8103–8122.

32 M. Shiraiwa, Y. Li, A. P. Tsimpidi, V. A. Karydis, T. Berkemeier, S. N. Pandis, J. Lelieveld, T. Koop and U. Pöschl, Global distribution of particle phase state in atmospheric secondary organic aerosols, *Nat. Commun.*, 2017, **8**, 1–7.

33 D. K. Farmer, M. E. Vance, J. P. D. Abbatt, A. Abeleira, M. R. Alves, C. Arata, E. Boedicker, S. Bourne, F. Cardoso-Saldã, R. Corsi, P. F. DeCarlo, A. H. Goldstein, V. H. Grassian, L. Hildebrandt Ruiz, J. L. Jimenez, T. F. Kahan, E. F. Katz, J. M. Mattila, W. W. Nazaroff, A. Novoselac, R. E. O'brien, V. W. Or, S. Patel, S. Sankhyan, P. S. Stevens, Y. Tian, M. Wade, C. Wang, S. Zhou and Y. Zhou, Overview of HOMEChem: House Observations of Microbial and Environmental Chemistry, *Environ. Sci. Process. Impacts*, 2019, **21**, 1280–1300.

34 C. Mohr, J. A. Huffman, M. J. Cubison, A. C. Aiken, K. S. Docherty, J. R. Kimmel, I. M. Ulbrich, M. Hannigan and J. L. Jimenez, Characterization of Primary Organic Aerosol Emissions from Meat Cooking, Trash Burning, and Motor Vehicles with High-Resolution Aerosol Mass Spectrometry and Comparison with Ambient and Chamber Observations, *Environ. Sci. Technol.*, 2009, **43**, 2443–2449.

35 C. Kaltsonoudis, E. Kostenidou, E. Louvaris, M. Psichoudaki, E. Tsiligiannis, K. Florou, A. Liangou and S. N. Pandis, Characterization of fresh and aged organic aerosol emissions from meat charbroiling, *Atmos. Chem. Phys.*, 2017, **17**, 7143–7155.

36 E. S. Robinson, P. Gu, Q. Ye, H. Z. Li, R. U. Shah, J. S. Apte, A. L. Robinson and A. A. Presto, Restaurant Impacts on Outdoor Air Quality: Elevated Organic Aerosol Mass from Restaurant Cooking with Neighborhood-Scale Plume Extents, *Environ. Sci. Technol.*, 2018, **52**, 9285–9294.

37 E. Reyes-Villegas, T. Bannan, M. Le Breton, A. Mehra, M. Priestley, C. Percival, H. Coe and J. D. Allan, Online Chemical Characterization of Food-Cooking Organic Aerosols: Implications for Source Apportionment, *Environ. Sci. Technol.*, 2018, **52**, 5308–5318.

38 Y. Zhao, M. Hu, S. Slanina and Y. Zhang, Chemical Compositions of Fine Particulate Organic Matter Emitted from Chinese Cooking, *Environ. Sci. Technol.*, 2007, **41**, 99–105.

39 A. L. Robinson, R. Subramanian, N. M. Donahue, A. Bernardo-Bricker and W. F. Rogge, Source Apportionment of Molecular Markers and Organic Aerosol. 3. Food Cooking Emissions, *Environ. Sci. Technol.*, 2006, **40**, 7820–7827.

40 J. J. Schauer, M. J. Kleeman, G. R. Cass and B. R. T. Simoneit, Measurement of Emissions from Air Pollution Sources. 4. C 1-C 27 Organic Compounds from Cooking with Seed Oils, *Environ. Sci. Technol.*, 2002, **36**, 567–575.

41 C. Mohr, P. F. DeCarlo, M. F. Heringa, R. Chirico, J. G. Slowik, R. Richter, C. Reche, A. Alastuey, X. Querol, R. Seco, J. Peñuelas, P. Peñuelas, J. L. Jiménez, M. Crippa, R. Zimmermann, U. Baltensperger and A. S. H. Prévôt, Identification and quantification of organic aerosol from cooking and other sources in Barcelona using aerosol mass spectrometer data, *Atmos. Chem. Phys.*, 2012, **12**, 1649–1665.

42 Y. Omelekhina, A. Eriksson, F. Canonaco, A. S. H. Prevot, P. Nilsson, C. Isaxon, J. Pagels and A. Wierzbicka, Cooking and electronic cigarettes leading to large differences between indoor and outdoor particle composition and concentration measured by aerosol mass spectrometry, *Environ. Sci. Process. Impacts*, 2020, **22**, 1382–1396.

43 K. L. Abdullahi, J. M. Delgado-Saborit and R. M. Harrison, Emissions and indoor concentrations of particulate matter and its specific chemical components from cooking: A review, *Atmos. Environ.*, 2013, **71**, 260–294.

44 S. Zhou, M. W. Forbes and J. P. D. Abbatt, Kinetics and Products from Heterogeneous Oxidation of Squalene with Ozone, *Environ. Sci. Technol.*, 2016, **50**, 11688–11697.

45 P. F. DeCarlo, J. R. Kimmel, A. Trimborn, M. J. Northway, J. T. Jayne, A. C. Aiken, M. Gonin, K. Fuhrer, T. Horvath, K. S. Docherty, D. R. Worsnop and J. L. Jimenez, Field-deployable, high-resolution, time-of-flight aerosol mass spectrometer, *Anal. Chem.*, 2006, **78**, 8281–8289.

46 M. R. Canagaratna, J. T. Jayne, J. L. Jimenez, J. D. Allan, M. R. Alfarra, Q. Zhang, T. B. Onasch, F. Drewnick, H. Coe, A. Middlebrook, A. Delia, L. R. Williams, A. M. Trimborn, M. J. Northway, P. F. DeCarlo, C. E. Kolb, P. Davidovits and D. R. Worsnop, Chemical and microphysical characterization of ambient aerosols with the aerodyne aerosol mass spectrometer, *Mass. Spec. Rev.*, 2007, **26**, 185–222.

47 E. Q. Walhout, H. Yu, C. Thrasher, J. M. Shusterman and R. E. O'Brien, Effects of Photolysis on the Chemical and Optical Properties of Secondary Organic Material Over Extended Time Scales, *ACS Earth Sp. Chem.*, 2019, **3**, 1226–1236.

48 P. F. DeCarlo, J. G. Slowik, D. R. Worsnop, P. Davidovits and J. L. Jimenez, Particle Morphology and Density Characterization by Combined Mobility and Aerodynamic Diameter Measurements. Part 1: Theory, *Aerosol Sci. Technol.*, 2004, **38**, 1185–1205.

49 E. F. Katz, H. Guo, P. Campuzano-Jost, D. A. Day, W. L. Brown, E. Boedicker, M. Pothier, D. M. Lunderberg, S. Patel, K. Patel, P. L. Hayes, A. Avery, L. H. Ruiz, A. H. Goldstein, M. E. Vance, D. K. Farmer, J. L. Jimenez and P. F. DeCarlo, Quantification of Cooking Organic Aerosol in the Indoor Environment using Aerodyne Aerosol Mass Spectrometers, *Aerosol Sci. Technol.*, submitted.

50 M. R. Canagaratna, J. L. Jimenez, J. H. Kroll, Q. Chen, S. H. Kessler, P. Massoli, L. Hildebrandt Ruiz, E. Fortner, L. R. Williams, K. R. Wilson, J. D. Surratt, N. M. Donahue, J. T. Jayne and D. R. Worsnop, Elemental ratio measurements of organic compounds using aerosol mass spectrometry: characterization, improved calibration, and implications, *Atmos. Chem. Phys.*, 2015, **15**, 253–272.

51 T. Braman, L. Dolvin, C. Thrasher, H. Yu, E. Q. Walhout and R. E. O'Brien, Fresh versus Photo-recalcitrant Secondary Organic Aerosol: Effects of Organic Mixtures on Aqueous Photodegradation of 4-Nitrophenol, *Environ. Sci. Technol. Lett.*, 2020, **7**, 248–253.

52 H. P. Dette, M. Qi, D. C. Schrö, A. Godt and T. Koop, Glass-Forming Properties of 3-Methylbutane-1,2,3-tricarboxylic Acid and Its Mixtures with Water and Pinonic Acid, *J. Phys. Chem. A*, 2014, **118**, 7024–7033.

53 M. D. Petters and S. M. Kreidenweis, A single parameter representation of hygroscopic growth and cloud condensation nucleus activity, *Atmos. Chem. Phys.*, 2007, **7**, 1961–1971.

54 Y. Li, A. Tasoglou, A. Liangou, K. P. Cain, L. Jahn, P. Gu, E. Kostenidou and S. N. Pandis, Cloud condensation nuclei activity and hygroscopicity of fresh and aged cooking organic aerosol, *Atmos. Environ.*, 2018, **176**, 103–109.

55 T. Koop, J. Bookhold, M. Shiraiwa and U. Pöschl, Glass transition and phase state of organic compounds: dependency on molecular properties and implications for secondary organic aerosols in the atmosphere, *Phys. Chem. Chem. Phys.*, 2011, **13**, 19238–19255.

56 C. A. Angell, Relaxation in liquids, polymers and plastic crystals-strong/fragile patterns and problems, *J. Non. Cryst. Solids*, 1991, **131**, 13–31.

57 N. E. Rothfuss and M. D. Petters, Influence of functional groups on the viscosity of organic aerosol, *Environ. Sci. Technol.*, 2016, **51**, 271–279.

58 M. Elser, R.-J. Huang, R. Wolf, J. G. Slowik, Q. Wang, F. Canonaco, G. Li, C. Bozzetti, K. R. Daellenbach, Y. Huang, R. Zhang, Z. Li, J. Cao, U. Baltensperger, I. El-Haddad and A. S. H. Prévôt, New insights into PM 2.5 chemical composition and sources in two major cities in China during extreme haze events using aerosol mass spectrometry, *Atmos. Chem. Phys.*, 2016, **16**, 3207–3225.

59 M. Crippa, I. El Haddad, J. G. Slowik, P. F. DeCarlo, C. Mohr, M. F. Heringa, R. Chirico, N. Marchand, J. Sciare, U. Baltensperger and A. S. H. Prévôt, Identification of marine and continental aerosol sources in Paris using high resolution aerosol mass spectrometry, *J. Geophys. Res. Atmos.*, 2013, **118**, 1950–1963.

60 *USDA Agricultural Research Service, Oil, soybean, nutrients*, https://fdc.nal.usda.gov/fdc-app.html#/food-details/748366/nutrients.

61 J. P. Reid, A. K. Bertram, D. O. Topping, A. Laskin, S. T. Martin, M. D. Petters, F. D. Pope and G. Rovelli, The viscosity of atmospherically relevant organic particles, *Nat. Commun.*, 2018, **9**, 956.

62 R. D. O'Brien, *Fats and Oils: Formulating and Processing for Applications*, CRC Press, 2009.

63 N. R. Gervasi, D. O. Topping and A. Zuend, A predictive group-contribution model for the viscosity of aqueous organic aerosol, *Atmos. Chem. Phys.*, 2020, **20**, 2987–3008.

64 J. Liu, H. Deng, P. S. J. Lakey, H. Jiang, M. Mekic, X. Wang, M. Shiraiwa and S. Gligorovski, Unexpectedly High Indoor HONO Concentrations Associated with Photochemical NO_2 Transformation on Glass Windows, *Environ. Sci. Technol.*, 2020, **54**, 15680–15688.

